Tensor-Based Efficient Multi-Interferer RFI Excision: Results Using Real-World Data

Tilahun Melkamu Getu[†‡], Wessam Ajib[‡], Omar A. Yeste-Ojeda[*], and René Jr. Landry[†]
[†]École de Technologie Supérieure (ÉTS), Montréal, QC, Canada
[‡]Université du Québec à Montréal (UQÀM), Montréal, QC, Canada
[*]National Radio Astronomy Observatory, Charlottesville, VA, USA
tilahun-melkamu.getu.1@ens.etsmtl.ca, ajib.wessam@uqam.ca, omar.yeste@gmail.com, and renejr.landry@etsmtl.ca

***Abstract*—Recently, we proposed a multi-linear subspace estimation and projection (MLSEP) algorithm for single-input multiple-output (SIMO) wireless communication systems that may suffer from multiple sources of radio frequency interference (RFI). Simulations corroborate a superior performance for MLSEP over the state-of-the-art projection-based RFI detection algorithms. To assess the efficacy of excision by MLSEP as well as the aforementioned state-of-the-art algorithms, this paper deploys a real-world data contaminated by multiple sources of RFI and conducts a performance assessment on such a data. Lastly, this assessment also demonstrates that MLSEP outperforms projection-based RFI excision algorithms, while effectively extracting the signal of interest from impinging RFIs.**

***Index Terms*—RFI excision, multi-linear subspace estimation, multi-linear projection, projection-based algorithms, real-world RFI contaminated data.**

I. Introduction

Intentional or unintentional radio frequency interference (RFI) is being prevalent in both terrestrial and satellite communications systems because of out of band emissions by nearby transmitters and harmonics, jamming, spoofing, and meaconing [1]–[3]. In particular, RFI is being increasingly common in microwave radiometry [4], radio astronomy [5], and satellite communications [6]. For instance, global navigation satellite systems and very small aperture terminal are increasingly suffering from RFI. In this respect, it is attested by [7] that 93% of the satellite industry suffer from interference. Moreover, RFI is prevalent in ultra-wideband communication systems for intentional and unintentional narrowband interferers [8], radar systems because of jammers [9], and cognitive radio communication systems for an imperfect spectrum sensing [10] and neighboring primary users emitting RFI [11].

In order to excise such a predominantly impinging RFI, efficient RFI detection and excision algorithms are needed. In this respect, the state-of-the-art encompasses several algorithms such as spectral [12], temporal [13], spectro-temporal [6], transformed domain-based [14], statistical [15], and spatial filtering-based [5], [16] RFI detection and excision algorithms. However, these algorithms tend to be inefficient and computationally complex, for they exhibit several non-linearities.

Having been inspired by the efficiency of tensor-based parameter estimators [17], [18], the multi-linear subspace estimation and projection (MLSEP) algorithm was proposed in [3] for single-input multiple-output (SIMO) systems suffering from a single source of RFI. It was demonstrated that the proposed MLSEP has an efficient RFI excision capability when compared with the subspace projection (SP) [16] and the cross subspace projection (CSP) [5] algorithms. Using oversampled antenna arrays, MLSEP was enhanced in [2], where a much better RFI excision was demonstrated when the oversampling factor gets larger. The MLSEP algorithm proposed in [3] was generalized in [1] to accommodate the case of several sources of RFI. In particular, MLSEP was deployed in [1] for efficient multi-interferer RFI (MI-RFI) excision in SIMO systems. For the MI-RFI setting, Monte-Carlo simulations also corroborate a significant RFI excision performance for MLSEP in comparison with the aforementioned projection-based RFI excision algorithms. When the perturbations get infinitesimally small, it was also proved in [1] that the limit of the root mean square excision error converges to zero for MLSEP faster than for SP.

So as to assess the efficacy of a real-word MI-RFI excision using the aforementioned algorithms, a simulation study which deploys a real-world RFI contaminated data was conducted and highlighted in [1]. The conducted simulation study is summarized as follows. First, we depicted the fast Fourier transforms (FFT) of a real-world RFI contaminated analog-to-digital converter (ADC) data received by one of the antennas of the Very Large Array (VLA) [19]. In so doing, we identified four impinging RFIs on the lower frequency component of the received ADC data. Second, the four RFIs were extracted using four properly designed and near-optimal *Kaiser window* bandpass filters. Third, the extracted RFIs were superimposed and additive white Gaussian noise (AWGN) was added to simulate different ranges of the interference-to-noise ratio (INR). Fourth, MLSEP, SP, and CSP algorithms were applied to the extracted RFIs which were contaminated by an AWGN. By doing so, the RFI excision efficacy of these algorithms was examined. At last, a spatial filtering of the received real-world RFI contaminated data was conducted and assessed.

The aforementioned highlighted study is subsequently detailed by this paper. Specifically, the contributions of this paper are itemized below.

- To extract a real-world MI-RFI, this paper designs four near-optimal Kaiser window bandpass filters.
- This paper demonstrates a real-world MI-RFI excision

978-15386-3652-7/18/$31.00 ©2018 IEEE

using MLSEP, SP, and CSP.
- When a relatively stationary MI-RFI impinges on the receiving antenna, this paper demonstrates a real-world SOI spatial filtering using MLSEP, SP, and CSP.

Following this introduction, Section II presents an overview of the MLSEP algorithm which is a tensor-based MI-RFI excision algorithm proposed in [1]. Section III interprets an MI-RFI contaminated VLA data which we received from The National Radio Astronomy Observatory (NRAO). Section IV outlines the MI-RFI excision and signal of interest (SOI) filtering setup. Thereafter, the respective results are reported in Section V and conclusions are drawn in Section VI.

II. Overview of the Tensor-Based MI-RFI Excision

In a nutshell, the MLSEP algorithm which was proposed for efficient MI-RFI excision in SIMO systems comprises three steps [1, Algorithm 1]:

- the MI-RFI subspace estimation using the MI-RFI subspace estimating tensor;
- the computation of the multi-linear projector rendering an efficient MI-RFI excision; and
- a multi-linear MI-RFI excision.

In MLSEP, W samples from each receiver antenna are stacked to render one highly structured vector. Such vectors are, in turn, horizontally concatenated to generate a matrix per a long-term interval (LTI). Using a higher-order singular value decomposition (SVD), the MI-RFI subspace tensor is estimated by deploying the multi-linear equivalent of the generated matrix. Having employed the estimated MI-RFI subspace tensor, the multi-linear projector which renders an efficient MI-RFI excision is computed. At last, a per LTI MI-RFI excision is conducted using the computed multi-linear projector.

Monte-Carlo simulations have corroborated a superior performance for MLSEP with respect to (w.r.t.) the performance of SP and CSP. The superiority was evident especially for sample starved settings and $N_R > \sum_{i=1}^{Q}(L_i+1)$, for N_R, L_i, and Q being the number of receive antennas, the channel order of the ith RFI, and the number of RFIs, respectively [1]. To assess the aforementioned superiority exhibited by MLSEP, further simulations have been conducted using a real-world MI-RFI contaminated data described underneath.

III. Interpretation of the Received VLA Data

To conduct an MI-RFI excision performance assessment on a real-world MI-RFI data, we received a real-world MI-RFI contaminated ADC data sampled at a sampling frequency of 2048 MHz. Having been received by one of the antennas of the VLA [19] of the NRAO, the ADC data was measured for maintenance purposes.

To identify the specific frequency bands that suffer from RFI, Fig. 1 depicts the absolute value of the FFT of the VLA data. For the same data, Fig. 2 depicts its magnified lower frequency component. As expected for the FFT of a real-valued signal [20], the spectrum is symmetric w.r.t. $f = 0$. Note that $f = 0$ corresponds to a sky frequency of 3988 MHz. Meanwhile, the ADC DC offset is observable at $f = 0$, $10\log_{10}|Y(f)|$ implies the magnitude of the FFT in dB, and the FFT *bins* are scaled w.r.t. the sampling frequency.

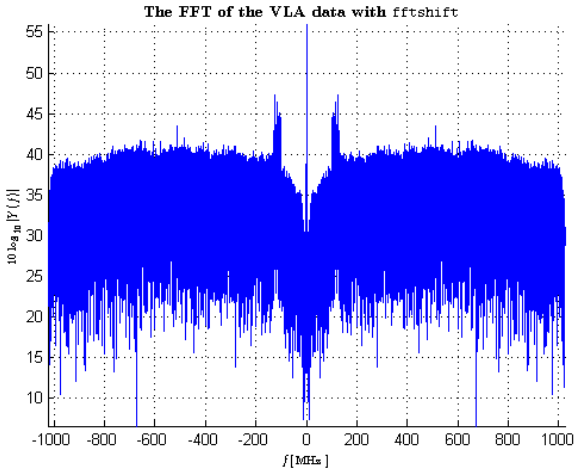

Fig. 1. The absolute value of the FFT of the VLA data.

As seen in Fig. 2, there are four RFIs in four subbands: 102.8 -107.2 MHz, 110.7-115 MHz, 115.2-118.8 MHz, and 123.9-127.5 MHz. These frequency bands plus the aforementioned sky frequency imply that the RFIs are emitted by satellites transmitting in the downlink of a C band [21, Table 1.3]. Note that these RFIs are superimposed to generate an MI-RFI. Because of the high directivity of the VLA antennas at a high frequency [19] and the received MI-RFI power, we assume that the aforementioned RFIs are received upon a line-of-sight propagation, i.e., $\{L_i\}_{i=1}^{4} = 0$ [3].

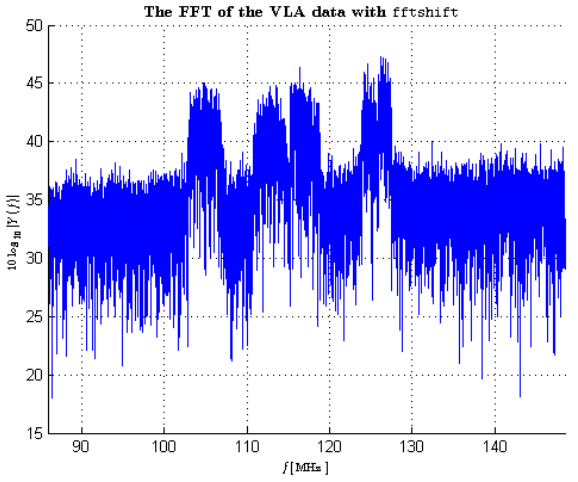

Fig. 2. The lower frequency component.

The four RFIs visible in Fig. 2 are going to be extracted using four near-optimal Kaiser window bandpass filters. By doing so, the RFIs would be superimposed rendering an input to the MI-RFI excision and SOI filtering assessment which employ the setup detailed subsequently.

IV. MI-RFI Excision and SOI Filtering Setup

In order to verify the efficacy of the MI-RFI excision using MLSEP, SP, and CSP, the four satellite RFIs which are visible in the aforementioned subbands should be extracted and superimposed. The extraction of the RFIs can be executed with the help of four properly designed bandpass filters. These filters can be designed to be either finite impulse response (FIR) or infinite impulse response filters. However, FIR filters are preferred to IIR filters provided that there is a requirement for a linear-phase characteristics within the passband of the filter [22]. As we desired to have filtered RFIs which exhibit linear-phase characteristics within the passband of the respective filters, we decided to design FIR bandpass filters. Accordingly, the overall setup boils down to the design of four bandpass filters which shall preferably employ near-optimal windows.

To design the four FIR bandpass filters, we have deployed the Kaiser window which is a near-optimal window as well as the most widely used and adjustable window [20], [23]. To continue, the first and second Kaiser window bandpass filters are designed to be odd length filters with passbands defined from 102.8-107.2 MHz and 110.7-115 MHz, respectively. Besides, they exhibit a 5% passband ripple, a 200 kHz wide stopbands to the left and right of the aforementioned subbands, and a stopband attenuation of 40 dB. As demonstrated by Fig. 3 which also displays the magnitude of the frequency response $|H(f)|$ exhibited by the designed filters, the first and second Kaiser window bandpass filters effectively extract the first two satellite RFIs.

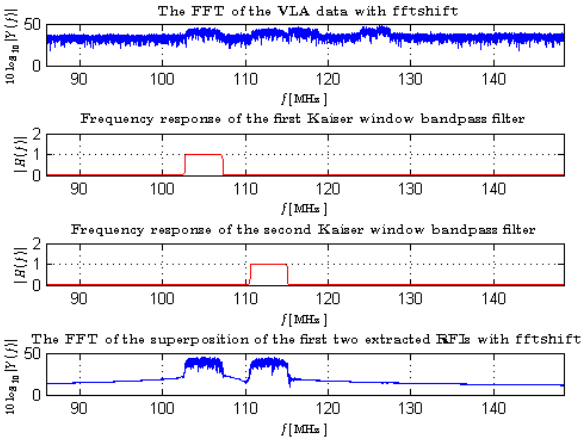

Fig. 3. Extraction of the first two RFIs.

Similarly, the third and fourth bandpass filters which, respectively, pass frequencies in the subbands 115.2-118.8 MHz and 123.9-127.5 MHz are also designed using a near-optimal Kaiser window bandpass filters. These filters also exhibit a 5% passband ripple, a 200 kHz wide stopbands to the left and right of the respective subbands, and a stopband attenuation of 40 dB. As corroborated by Fig. 4, these Kaiser window bandpass filters effectively extract the third and fourth satellite RFIs. Through a superposition of the four extracted RFIs, the MI-RFI impinging on one of the antennaas of the VLA is obtained. However, we need to obtain the MI-RFI received by the remaining $(N_R - 1)$ antennas, as the proposed projection algorithms rely on multiple antennas.

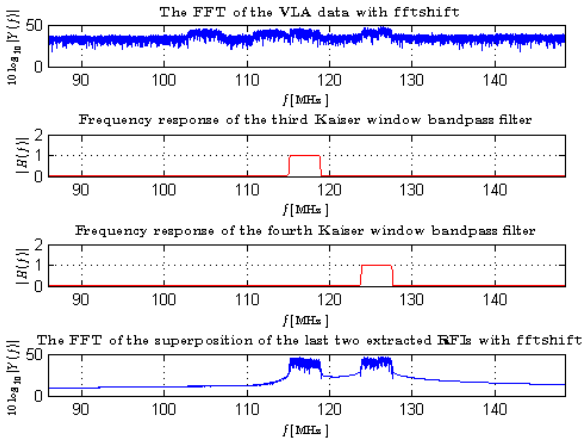

Fig. 4. Extraction of the last two RFIs.

To generate the data for the remaining antennas, we assume, for simplicity but without loss of generality, a uniform linear array (ULA) and angle of arrival such that a delay of one sample becomes evident between two neighboring antennas. From the extracted MI-RFI, the MI-RFI for the remaining $(N_R - 1)$ antennas is generated by deploying the aforementioned geometry. In order to assess the performance of the aforementioned algorithms for the ranges of the INR, we have added an AWGN of power σ^2 to the extracted MI-RFI of all antennas and defined INR denoted by γ_{inr} as

$$\gamma_{inr} = 10 \log_{10} \frac{||\boldsymbol{V}||_F^2}{N N_R \sigma^2}, \tag{1}$$

where $||\cdot||_F$ implies Frobenius norm, N denotes the number of short-term intervals per LTI, and $\boldsymbol{V}$ is a matrix made of the horizontal concatenation of the highly structured vectors that are made by stacking W extracted MI-RFI samples of the N_R antennas. Note that $\boldsymbol{V}$ is the matrix, made of the extracted MI-RFI and contaminating AWGN—arranged as in [1, eq. (7)]. The extracted MI-RFI samples are then grouped into several LTIs which comprise $N_{\text{tot}} = NW$ samples. Similar to the system model of [1], we henceforth assume a relatively stationary MI-RFI w.r.t. the SOI.

By deploying the extracted MI-RFI samples in this arrangement, MLSEP is simulated by computing the multi-linear projector [1, eq. (13)] as per [1, Algorithm 1]. SP is simulated by taking the dominant eigenvalues of the space-time correlation matrix, as in [3]. On the other hand, CSP is simulated by taking the SVD of the space-time crosscorrelation matrix made of the highly structured vectors of N_R antennas and N_R^a auxiliary antennas, as in [5].

For our further assessment, we have considered the VLA spectrum apart from the four extracted RFIs as the SOI

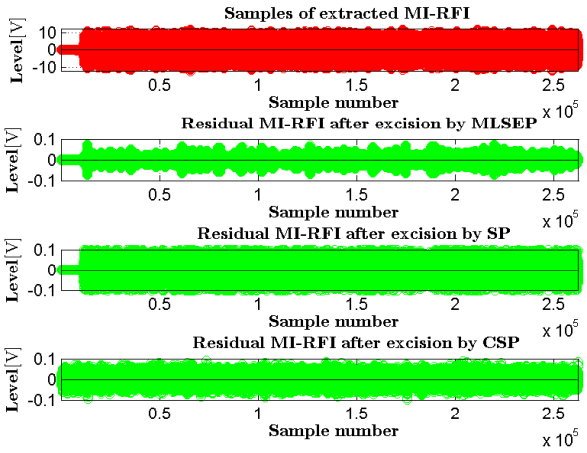

Fig. 5. MI-RFI excision with the VLA data.

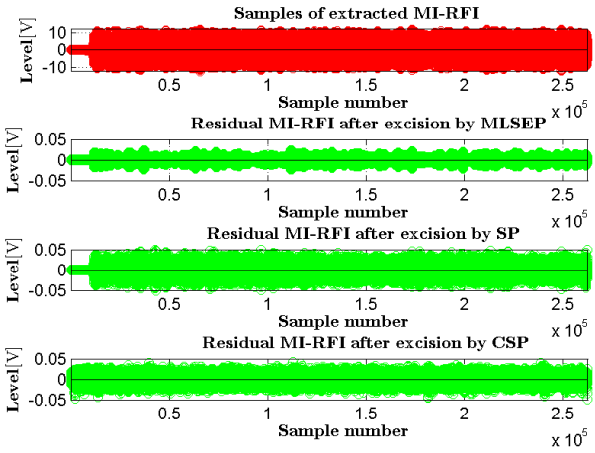

Fig. 6. MI-RFI excision with the VLA data: $\gamma_{inr} = 30$ dB.

spectrum. In order to further justify the efficacy of the MI-RFI excision, we are going to plot the FFT of the VLA data which was spatially filtered by MLSEP, SP, and CSP. In this respect, we generate the VLA data for the remaining (N_R-1) antennas by deploying the aforementioned ULA. Having employed the multi-linear projector computed above, we have conducted a spatial filtering using MLSEP on the received, stacked, and horizontally concatenated VLA data of the N_R antennas. In particular, such a spatial filtering is conducted for a relatively stationary MI-RFI assumed in [1]. Using the aforementioned correlation and crosscorrelation matrices, projection matrices of SP and CSP are computed. Thereafter, the vertically stacked and horizontally concatenated VLA data is spatially filtered using SP and CSP, also for the aforementioned MI-RFI.

Assessment parameters	Assigned value
$[Q, W]$	$[4, 5]$
N_{tot}	800
$[N_R, N_R^a]$	$[10, 6]$
γ_{inr}	20 dB

TABLE I
ASSESSMENT PARAMETERS UNLESS OTHERWISE MENTIONED.

V. RESULTS

The performance assessment on an MI-RFI contaminated VLA data leading to the results in Figs. 5-8 has been conducted using the parameters of Table I. Note that the reported results are for the given VLA antenna; considered the first antenna.

Figs. 5-7 demonstrate the MI-RFI excision by MLSEP, SP, and CSP, along with the extracted MI-RFI samples and their FFT. Having realized that the received power is proportional to the squared amplitude, the average residual MI-RFI power after the MLSEP excision is less than one-fourth of the average residual MI-RFI power after an SP or CSP excision, as corroborated by Figs. 5 and 6. These plots also attest that the average residual MI-RFI power decreases with the increment

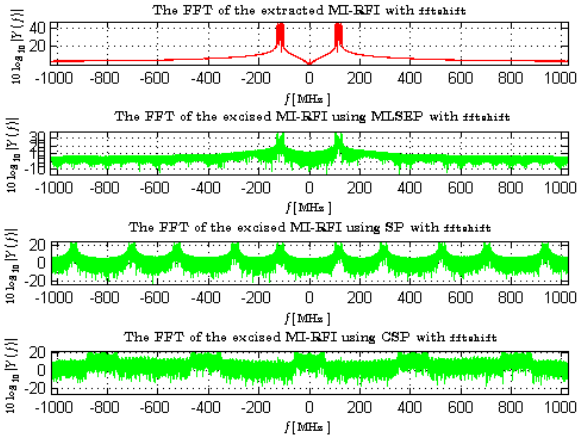

Fig. 7. The FFT of an MI-RFI excision with the VLA data.

of INR. This is evident for the fact that a larger INR results in a better estimation of the MI-RFI subspace and hence a more efficient MI-RFI excision. Meanwhile, Fig. 7 showcases an almost flat spectrum for an MI-RFI excision using MLSEP when compared with the non-flat spectra of SP and CSP. This implies the efficacy of excision using MLSEP, as it is also demonstrated by an approximately 10 dB excision of the extracted MI-RFI spectrum.

On the other hand, Fig. 8 depicts the FFT of the spatially filtered VLA data using MLSEP, SP, and CSP, along with the FFT of the received VLA data. As it is evident from Fig. 8, both SP and CSP render almost flat spectra in the low-frequency ranges of 0-130 MHz, unlike the spectrum of the VLA data. On the contrary, the spectrum of the VLA data after an MI-RFI spatial filtering by MLSEP produces a spectrum in the 0-130 MHz whose envelope almost follows that of the SOI, while excising the MI-RFI visibly. Apart from the MI-RFI contaminated subbands, the generated spectrum after an MLSEP filtering guarantees a flat spectrum pretty much like that of the original SOI spectrum.

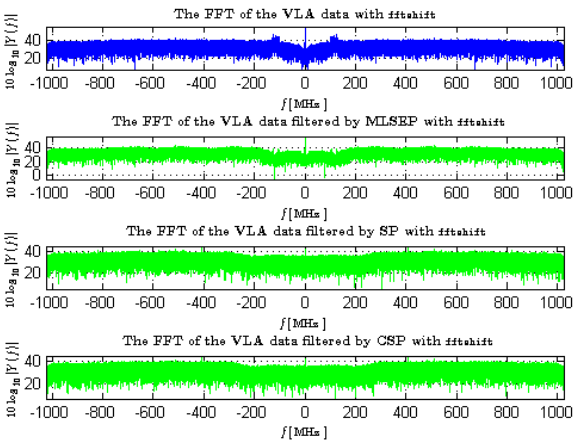

Fig. 8. The FFT of a spatially filtered VLA data.

VI. Conclusions

By deploying a real-world MI-RFI contaminated data, this paper has investigated the efficacy of MI-RFI excision using MLSEP, SP, and CSP. Near-optimal Kaiser window bandpass filters have been designed and deployed to extract each of the RFIs which are superimposed to render the interfering MI-RFI. On such a real-world RFI contaminated data in a multi-antenna setting, MLSEP, SP, and CSP are applied to assess their real-world MI-RFI excision efficacy.

Performance assessment on the aforementioned multi-antenna real-world data corroborates that the approximated residual MI-RFI power after the MLSEP excision is less than one-fourth of the approximated residual MI-RFI power after an excision by SP and CSP. It is also corroborated that filtering using MLSEP tends to keep the SOI spectrum, while efficiently excising the extracted MI-RFI. Following the performance of MLSEP in the excision of broadband MI-RFI reported in [1] and this performance assessment on a real-world MI-RFI contaminated data, it can be concluded that the proposed MLSEP algorithm efficiently excises any MI-RFI, while preserving the SOI.

Acknowledgments

The authors acknowledge the AVIO-601 Project for the provided funding and Alan Erickson of the National Radio Astronomy Observatory[1] for facilitating the RFI data.

References

[1] T. M. Getu, W. Ajib, and O. A. Yeste-Ojeda, "Tensor-based efficient multi-interferer RFI excision algorithms for SIMO systems," *IEEE Trans. Commun.*, vol. 65, no. 7, pp. 3037–3052, Jul. 2017.

[1]The National Radio Astronomy Observatory is a National Science Foundation facility operated under a cooperative agreement by Associated Universities, Inc.

[2] T. M. Getu, W. Ajib, and R. Landry, "Oversampling-based algorithm for efficient RF interference excision in SIMO systems," in *Proc. IEEE Global Conf. on Signal and Inform. Process. (IEEE GlobalSIP)*, Washington DC, DC, USA, Dec. 2016, pp. 1423–1427.

[3] T. M. Getu, W. Ajib, and O. A. Yeste-Ojeda, "Multi-linear subspace estimation and projection for efficient RFI excision in SIMO systems," in *Proc. IEEE Global Conf. on Signal and Inform. Process. (IEEE GlobalSIP)*, Orlando, FL, USA, Dec. 2015, pp. 1397–1401.

[4] S. Misra, P. Mohammed, B. Guner, C. Ruf, J. Piepmeier, and J. Johnson, "Microwave radiometer radio-frequency interference detection algorithms: A comparative study," *IEEE Trans. Geosci. Remote Sens.*, vol. 47, no. 11, pp. 3742–3754, Nov. 2009.

[5] B. Jeffs, L. Li, and K. F. Warnick, "Auxiliary antenna-assisted interference mitigation for radio astronomy arrays," *IEEE Trans. Signal Process.*, vol. 53, no. 2, pp. 439–451, Feb. 2005.

[6] D. Borio, L. Camoriano, S. Savasta, and L. Lo Presti, "Time-frequency excision for GNSS applications," *IEEE Syst. J.*, vol. 2, no. 1, pp. 27–37, Mar. 2008.

[7] Newtec and IRG, "93% of the industry suffers from satellite interference," Sept. 2013. [Online]. Available: http://www.newtec.eu/article/release/93-of-the-industry-suffers-from-satellite-interference

[8] K. Shi, Y. Zhou, B. Kelleci, T. W. Fischer, E. Serpedin, and A. l. Karsilayan, "Impacts of narrowband interference on OFDM-UWB receivers: Analysis and mitigation," *IEEE Trans. Signal Process.*, vol. 55, no. 3, pp. 1118–1128, Mar. 2007.

[9] A. De Maio and D. Orlando, "Adaptive radar detection of a subspace signal embedded in subspace structured plus Gaussian interference via invariance," *IEEE Trans. Signal Process.*, vol. 64, no. 8, pp. 2156–2167, Apr. 2016.

[10] T. M. Getu, W. Ajib, and O. A. Yeste-Ojeda, "Efficient semi-blind channel estimators for SIMO systems suffering from broadband RFI," in *Proc. IEEE Int. Conf. on Ubiquitous Wireless Broadband (IEEE ICUWB)*, Montreal, QC, Canada, Oct. 2015.

[11] A. A. A. Boulogeorgos, N. D. Chatzidiamantis, and G. K. Karagiannidis, "Spectrum sensing with multiple primary users over fading channels," *IEEE Commun. Lett.*, vol. 20, no. 7, pp. 1457–1460, Jul. 2016.

[12] B. Guner, J. Johnson, and N. Niamsuwan, "Time and frequency blanking for radio-frequency interference mitigation in microwave radiometry," *IEEE Trans. Geosci. Remote Sens.*, vol. 45, no. 11, pp. 3672–3679, Nov. 2007.

[13] J. T. Johnson and S. W. Ellingson, "Examination of a simple pulse blanking technique for RFI mitigation," *Radio Sci.*, vol. 40, no. 5, p. RS5S03, Jun. 2005.

[14] F. Dovis, L. Musumeci, N. Linty, and M. Pini, "Recent trends in interference mitigation and spoofing detection," *Int. J. of Embedded and Real-Time Commun. Systems*, vol. 3, no. 3, pp. 1–17, Jul./Sep. 2012.

[15] C. Ruf, S. Gross, and S. Misra, "RFI detection and mitigation for microwave radiometry with an agile digital detector," *IEEE Trans. Geosci. Remote Sens.*, vol. 44, no. 3, pp. 694–706, Mar. 2006.

[16] S. van der Tol and A.-J. van der Veen, "Performance analysis of spatial filtering of RF interference in radio astronomy," *IEEE Trans. Signal Process.*, vol. 53, no. 3, pp. 896–910, Mar. 2005.

[17] F. Roemer, M. Haardt, and G. Del Galdo, "Analytical performance assessment of multi-dimensional matrix- and tensor-based ESPRIT-type algorithms," *IEEE Trans. Signal Process.*, vol. 62, no. 10, pp. 2611–2625, May 2014.

[18] M. Haardt, F. Roemer, and G. Del Galdo, "Higher-order SVD-based subspace estimation to improve the parameter estimation accuracy in multidimensional harmonic retrieval problems," *IEEE Trans. Signal Process.*, vol. 56, no. 7, pp. 3198–3213, Jul. 2008.

[19] NRAO, "Very Large Array of The National Radio Astronomy Observatory." [Online]. Available: http://www.vla.nrao.edu/

[20] A. V. Oppenheim and R. W. Schafer, *Discrete-Time Signal Processing*, 3rd ed. Upple Saddle River, NJ, USA: Pearson Higher Education, 2010.

[21] G. Maral and M. Bousquet, *Satellite Communications Systems: Systems, Techniques and Technology*, 5th ed. Hoboken, NJ, USA: Wiley, 2009.

[22] J. G. Proakis and D. K. Manolakis, *Digital Signal Processing*, 4th ed. Upper Saddle River, NJ, USA: Prentice-Hall, 2006.

[23] S. K. Mitra, *Digital Signal Processing: A Computer-Based Approach*, 2nd ed. New York, NY, USA: McGraw-Hill, 2001.